

An endoscopic system adopting a liquid crystal lens with an electrically tunable depth-of-field

Hung-Shan Chen, and Yi-Hsin Lin*

Department of Photonics, National Chiao Tung University, 1001 Ta Hsueh Rd., Hsinchu 30010, Taiwan

*yilin@mail.nctu.edu.tw

<http://www.cc.nctu.edu.tw/~yilin>

Abstract: Conventional endoscopic systems consisting of several solid lenses suffer from a fixed and limited depth-of-field (DOF). For practical applications, conventional endoscopes mechanically change the distance between the solid lenses of a lens module in order to change the focusing plane and DOF to see clearly in a scene. In this paper, we demonstrate an electrically tunable endoscopic system adopting a liquid crystal lens. By means of tunable focusing properties of the LC lens as a positive lens and a negative lens, the object at different objective distances can be imaged to the image sensor clearly and the corresponding depth-of-field can also help to enlarge the total spatial depth perception in a scene. The optical mechanism is discussed. In the experiments, under adjustment of three discrete lens powers of the LC lens, the viewing range or total spatial depth perception of the endoscopic system is from 76.4 mm to 12.4 mm which is 2x improved compared to the conventional one without LC lens. We believe this study can be extended to the applications of industrial and medical endoscopes.

©2013 Optical Society of America

OCIS codes: (230.3720) Liquid-crystal devices; (230.2090) Electro-optical devices.

References and links

1. M. Q. Yang, S. W. Huang, W. K. Su, H. M. Feng, Z. Y. Chen, H. M. Wu, and Y. T. Kuo, "Optimizing the depth of field for short object distance of capsule endoscope," Proc. SPIE **6859**, 68591Q, 68591Q-7 (2008).
2. M. Katz, *Introduction to Geometrical Optics* (World Scientific Publishing Co. Pte. Ltd., 2002).
3. P. Rol, R. Jenny, D. Beck, F. Frankhauser, and P. F. Niederer, "Optical properties of miniaturized endoscopes for ophthalmic use," Opt. Eng. **34**(7), 2070–2077 (1995).
4. S. Kuiper, "Electrowetting-based liquid lenses for endoscopy," Proc. SPIE **7930**, 793008, 793008-8 (2011).
5. X. Zeng, C. T. Smith, J. C. Gould, C. P. Heise, and H. Jiang, "Fiber endoscopes utilizing liquid tunable-focus microlenses actuated through infrared light," J. of Microelectromechanical Systems **20**(3), 583–593 (2011).
6. S. W. Seo, S. Han, J. H. Seo, W. B. Choi, and M. Y. Sung, "Liquid lens module with wide field-of view and variable focal length," Electronic Mater. Lett. **6**(4), 141–144 (2010).
7. S. W. Seo, S. Han, J. H. Seo, Y. M. Kim, M. S. Kang, N. K. Min, W. B. Choi, and M. Y. Sung, "Microelectromechanical-system-based variable-focus liquid lens for capsule endoscopes," Jpn. J. Appl. Phys. **48**(5), 052404 (2009).
8. Y. H. Lin and H. S. Chen, "Electrically tunable-focusing and polarizer-free liquid crystal lenses for ophthalmic applications," Opt. Express **21**(8), 9428–9436 (2013).
9. H. C. Lin and Y. H. Lin, "A fast response and large electrically tunable-focusing imaging system based on switching of two modes of a liquid crystal lens," Appl. Phys. Lett. **97**(6), 063505 (2010).
10. H. C. Lin and Y. H. Lin, "An electrically tunable focusing pico-projector adopting a liquid crystal lens," Jpn. J. Appl. Phys. **49**(10), 102502 (2010).
11. Y. H. Lin, M. S. Chen, and H. C. Lin, "An electrically tunable optical zoom system using two composite liquid crystal lenses with a large zoom ratio," Opt. Express **19**(5), 4714–4721 (2011).
12. H. C. Lin, N. Collings, M. S. Chen, and Y. H. Lin, "A holographic projection system with an electrically tuning and continuously adjustable optical zoom," Opt. Express **20**(25), 27222–27229 (2012).
13. Y. H. Lin, H. S. Chen, H. C. Lin, Y. S. Tsou, H. K. Hsu, and W. Y. Li, "Polarizer-free and fast response microlens arrays using polymer-stabilized blue phase liquid crystals," Appl. Phys. Lett. **96**(11), 113505 (2010).
14. H. Gross, H. Zügge, M. Peschka, and F. Blechinger, *Handbook of Optical Systems: Aberration Theory and Correction of Optical Systems* (WILEY-VCH, 2007, Vol. 3).
15. H. S. Chen, and Y. H. Lin, "An electrically tunable endoscopic system by adding a liquid crystal lens to enlarge and shift depth-of field," SPIE **8828** (2013).

16. B. Wang, M. Ye, and S. Sato, "Liquid crystal lens with focal length variable from negative to positive values," *IEEE Photon. Technol. Lett.* **18**(1), 79–81 (2006).
17. M. Ye, B. Wang, M. Uchida, S. Yanase, S. Takahashi, M. Yamaguchi, and S. Sato, "Low-voltage-driving liquid crystal lens," *Jpn. J. Appl. Phys.* **49**(10), 100204 (2010).
18. H. Ren and S. T. Wu, *Introduction to Adaptive Lenses* (John Wiley & Sons, 2012).
19. H. C. Lin, M. S. Chen, and Y. H. Lin, "A review of electrically tunable focusing liquid crystal lenses," *Trans. Electr. Electron Mater.* **12**(6), 234–240 (2011).
20. H. C. Lin and Y. H. Lin, "An electrically tunable focusing liquid crystal lens with built-in planar polymeric lens," *Appl. Phys. Lett.* **98**(8), 083503 (2011).
21. R. El-Maksoud, L. Wang, J. M. Sasian, and V. S. Valencia, "Depth of field estimation: theory, experiment, and application," *Proc. SPIE* **7429**, 74290W, 74290W-12 (2009).
22. P. Valley, D. L. Mathine, M. R. Dodge, J. Schwiegerling, G. Peyman, and N. Peyghambarian, "Tunable-focus flat liquid-crystal diffractive lens," *Opt. Lett.* **35**(3), 336–338 (2010).
23. H. Ren, S. Xu, Y. Liu, and S. T. Wu, "Switchable focus using a polymeric lenticular microlens array and a polarization rotator," *Opt. Express* **21**(7), 7916–7925 (2013).
24. H. C. Lin and Y. H. Lin, "An electrically tunable-focusing liquid crystal lens with a low voltage and simple electrodes," *Opt. Express* **20**(3), 2045–2052 (2012).
25. H. Ren and S. T. Wu, "Inhomogeneous nanoscale polymer-dispersed liquid crystals with gradient refractive index," *Appl. Phys. Lett.* **81**(19), 3537–3539 (2002).
26. D. E. Lucchetta, R. Karapinar, A. Manni, and F. Simoni, "Phase-only modulation by nanosized polymer-dispersed liquid crystals," *J. Appl. Phys.* **91**(9), 6060–6065 (2002).
27. Y. H. Lin, H. Ren, and S. T. Wu, "Polarisation-independent liquid crystal devices," *Liquid Crystals Today* **17**(1-2), 2–8 (2008).
28. H. Ren, Y. H. Lin, Y. H. Fan, and S. T. Wu, "Polarization-independent phase modulation using a polymer-dispersed liquid crystal," *Appl. Phys. Lett.* **86**(14), 141110 (2005).
29. Y. H. Lin, H. Ren, Y. H. Fan, Y. H. Wu, and S. T. Wu, "Polarization-independent and fast-response phase modulation using a normal-mode polymer-stabilized cholesteric texture," *J. Appl. Phys.* **98**(4), 043112 (2005).
30. H. Ren, Y. H. Lin, C. H. Wen, and S. T. Wu, "Polarization-independent phase modulation of a homeotropic liquid crystal gel," *Appl. Phys. Lett.* **87**(19), 191106 (2005).
31. Y. Huang, C. H. Wen, and S. T. Wu, "Polarization-independent and submillisecond response phase modulators using a 90° twisted dual-frequency liquid crystal," *Appl. Phys. Lett.* **89**(2), 021103 (2006).
32. Y. H. Lin, H. Ren, Y. H. Wu, Y. Zhao, J. Y. Fang, Z. Ge, and S. T. Wu, "Polarization-independent liquid crystal phase modulator using a thin polymer-separated double-layered structure," *Opt. Express* **13**(22), 8746–8752 (2005).
33. H. Ren, Y. H. Lin, and S. T. Wu, "Polarization-independent and fast-response phase modulators using double-layered liquid crystal gels," *Appl. Phys. Lett.* **88**(6), 061123 (2006).
34. Y. H. Lin and Y. S. Tsou, "A polarization independent liquid crystal phase modulation adopting surface pinning effect of polymer dispersed liquid crystals," *J. Appl. Phys.* **110**(11), 114516 (2011).
35. Y. H. Lin, M. S. Chen, W. C. Lin, and Y. S. Tsou, "A polarization-independent liquid crystal phase modulation using polymer-network liquid crystals in a 90 degree twisted cell," *J. Appl. Phys.* **112**(2), 024505 (2012).
36. Y. S. Tsou, Y. H. Lin, and A. C. Wei, "Concentrating Photovoltaic System Using a Liquid Crystal Lens," *IEEE Photon. Technol. Lett.* **24**(24), 2239–2242 (2012).

1. Introduction

An endoscope is an important tool for medical diagnosis. In general, three main types of endoscopic systems are used: rigid endoscopes, flexible endoscopes and capsule endoscopes. Rigid endoscopes consisting of a set of lens modules and an image sensor are commonly used in the clinic examinations, such as gynecology and laparoscopy for internal medicine [1]. In the conventional endoscopic system, the depth-of-field (DOF), the distance between the nearest and farthest objects in a scene that appears clear in an image, is fixed and limited due to the fixed focusing properties of lens modules of endoscopes. The depth-of-field and depth-of-focus are the acceptable displacements in the focus plane and image plane, respectively [2]. In order to see the objects in a scene clearly, doctors have to move around the endoscope while the examinations and it makes patients uncomfortable. A lens module with a voice coil motor (VCM) which can mechanically change the distance between the solid lenses of a lens module in the endoscope is a way to change the DOF of the endoscope. However, the lens module with VCM for endoscopes is bulky and especially not suitable for the medical applications. A lens module with a large F-number can be adopted to enlarge DOF [3]. Nevertheless, the power density or irradiance (Watt/m^2) of the incoming light decreases as well as the spatial resolution reduces. Recently, many researchers proposed an endoscopic system adopting a liquid lens in order to change the focal plane of the endoscope [4–7]. To image the objects in the scene, the liquid lens changes the focal length continuously by

changing the curvature of the interface between two fluids. However, the reflection resulting from the liquid-liquid interface causes the decrease of the spatial resolution and the liquid lens is also bulky owing to the change of fluidic volume in order to adjust the curvature of the liquid lens. Besides, the previous literatures only discussed the focusing properties in endoscopic system using a liquid lens. In fact, tunable focusing lenses cannot only image the areas of interest but also obtain different spatial depth perception which means depth-of-field. However, the effect of the depth-of-field in the endoscopic system with an electrically tunable lens has not been discussed yet. In addition, the electrically tunable focusing liquid crystal (LC) lenses based on changing the spatial distribution of the effective refractive indices are developed many years and the performances of the LC lenses are also promising in many applications, such as pico projectors, imaging system for cell phones, and ophthalmic lenses [8–13]. Compared to the liquid lenses, the advantages of LC lenses are 1) no reflection from the curved liquid-liquid interface, 2) anti-reflection can be coated on the glass substrates, 3) the aperture size is not limited by the surface tension at liquid-liquid interface, especially for the small aperture size. In this paper, an electrically tunable endoscopic system by adopting a LC lens with a large viewing range or spatial depth perception is demonstrated. The liquid crystal lens with an operation of two modes, the positive and negative lenses, cannot only image the object of interest but also adjust the depth-of-field of the endoscopic system. By selecting three discrete tunable focal lengths of the LC lens, both of the shifts of the focal lengths and corresponding DOFs can help the endoscopic system to image the object from 76.4 mm to 12.4 mm without continuously changing the focal lengths of the LC lens. The optical mechanism of DOF in such an electrically tunable endoscopic system is investigated and discussed. The concept we proposed can also be applied to all kind of LC lenses as long as the LC lenses exhibit capability of operation of the positive lens and the negative lens. We believe this study can provide not only a guideline for designing active optical components for endoscopic systems but also can be extended in the applications of both industrial and medical endoscopes.

2. Operating principles and sample preparation

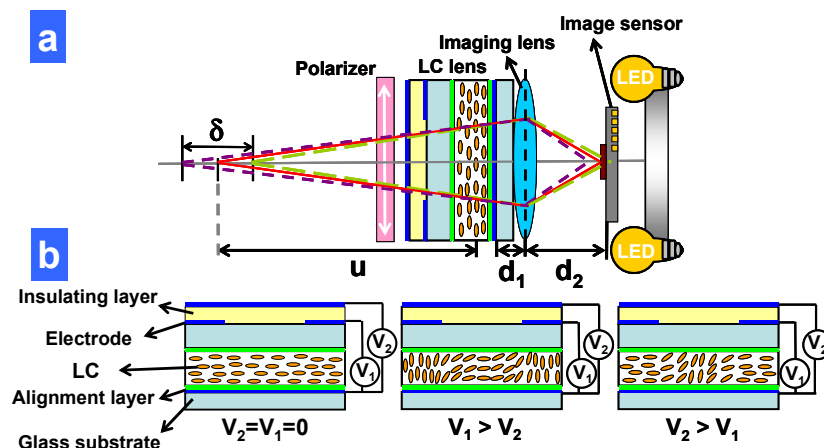


Fig. 1. (a) The illustration of the endoscopic system adopting a LC lens. The white arrow is the transmissive axis of the polarizer. (b) The structure of the LC lens in (a). When $V_2 = V_1 = 0$, lens power of the LC lens is zero. When $V_1 > V_2$, the LC lens is a positive lens and the lens power is positive. When $V_2 > V_1$, the LC lens is a negative lens and the lens power is negative.

The operating principles of the endoscopic system adopting a liquid crystal (LC) lens is illustrated in Figs. 1(a) and 1(b). The system consists of a polarizer, a LC lens, an imaging lens, light emitting diodes (LEDs) and an image sensor. The imaging lens is actually a set of lenses, or so-called lens module. The LEDs are to help see the objects. The object at an

objective distance (u) is imaged to the image sensor. Based on the image formation, the objective distance (u), the distance between the object and the LC lens, can be expressed as [8]:

$$u(V) = \frac{1}{P_{LC}(V) + P_{sys}}, \quad (1)$$

where V is the applied voltage of the LC lens, and $P_{LC}(V)$ is the voltage dependent lens power of the LC lens. The lens power is defined as the inverse of the focal length. In Eq. (1), P_{sys} is [7]:

$$P_{sys} = -\frac{1}{\frac{d_1}{n} + \frac{1}{P_s - \frac{1}{d_2}}}, \quad (2)$$

where d_1 is the distance between the LC lens and the imaging lens which approximately equals to the thickness of the glass substrate, n is the refractive index of the glass substrate, P_s is the lens power of the imaging lens, and d_2 is the distance between the imaging lens and the image sensor. When the objective distance changes a little ($\sim \pm \delta/2$), the resolution of the image on the image sensor is still acceptable. Such a tolerance of the objective distance (δ) is defined as depth of field (DOF) [2,14] δ is written in Eq. (3) [15]:

$$\delta(V) = \frac{2 \times B \times (u(V) - q) \times D_s'}{D_s'^2 - B^2}, \quad (3)$$

where D_s' is effective aperture size of the entrance pupil, B is the acceptable blur diameter which also means DOF depends on the resolution of the image sensor, q is the distance between the entrance pupil of the system and the LC lens. DOF or δ can be expressed in Eq. (4) after we put the $u(V)$ in Eq. (1) into Eq. (3) under an assumption of $D_s \gg B$ which is generally true:

$$\delta(V) \approx \frac{2B \times (u(V) - q)}{(\frac{q}{n} \times d_1) \times D_s} \approx \frac{2 \times n \times B}{d_1 \times D_s} \times \left(\frac{u(V)}{q} - 1 \right). \quad (4)$$

In the endoscopic system for the medical applications, u (~ 30 to 60 mm) is much larger than $|q|$ ($\sim |-0.45\text{mm}|$ to $|-0.46\text{mm}|$). (i.e. $u \gg q$) As a result, q can be seen as a constant. As a result, $\delta(V)$ in Eq. (4) is proportional to $B \times u(V)$ and can be expressed as:

$$\delta(V) \propto B \times u(V) = \frac{B}{P_{LC}(V) + P_{sys}}. \quad (5)$$

According to Eq. (5) and Eq. (1), the object can be imaged to the image sensor when the object is placed at a certain location with a variation of distance δ when the LC lens is off (i.e. $P_{LC} = 0$). When the LC lens is activated (i.e. $P_{LC} \neq 0$), we can electrically adjust the lens power of the LC lens in order to see the clear image when the objective distance changes. In Eq. (1), when the LC lens is a positive lens (i.e. $P_{LC}(V) > 0$), the objective distance decreases with an increase of the lens power which means the endoscopic system can see nearer. When the LC lens is a negative lens (i.e. $P_{LC}(V) < 0$), the objective distance increases with a decrease of the lens power which means the endoscopic system can see further. Moreover, the DOF is proportional to the objective distance. This also indicates we are able to adjust the lens power discretely to change the objective distance. Then both of the objective distance as well as the corresponding DOF are able to help the system to see the objects in the entire objective range.

Therefore, we can realize an endoscopic system within a large spatial perception by adopting a LC lens which is operated as a positive lens and a negative lens.

To demonstrate the concept, we adopted a LC lens based on two-voltage structure which can be operated as a positive lens and a negative lens, as illustrated in Fig. 1(b) [8–11,16,17]. The structure of the LC lens consists of three layers of indium tin oxide (ITO) as electrodes, two glass substrates of thickness 0.7 mm, a layer of NOA81 (Norland Optical Adhesive) with thickness of 25 μm as an insulating layer, a LC layer with thickness of 50 μm , and two alignment layers of PVA (Polyvinylalcohol) which are mechanically buffed to align LC directors. The rubbing directions of two alignment layers are anti-parallel. One of the ITO layer was etched with a hole with a diameter of 2 mm in order to provide an inhomogeneous electric field to LC directors. The nematic LC mixture MLC-2070 (Merck, MLC-2070, $\Delta n = 0.26$ for $\lambda = 589.3$ nm at 20°C) was used. The voltage applied between the hole-patterned ITO and the bottom ITO layer was defined as V_1 . The other applied voltage was defined as V_2 , as shown in Fig. 1(b). When $V_1 = V_2 = 0$, the lens power of the LC lens is zero. When $V_1 > V_2$, the LC directors near the rim of the aperture are reoriented more by the electric fields and then the LC lens is operated as a positive lens. When $V_1 < V_2$, the LC directors near the center of the aperture are reoriented more and then the LC lens is operated as a negative lens. By changing the magnitude of V_1 and V_2 , the focal length of the LC lens is electrically switchable. The structure of the LC lenses is not limited in the structure shown in Figs. 1(a) and 1(b). In fact, the concept here can also be applied to all kind of LC lenses when the LC lenses can be operated as both of the positive lens and the negative lens.

3. Experimental results and discussions

To observe the phase profile of the LC lens, we observed the image of the LC lens when the LC lens was placed between two crossed polarizers with the rubbing direction of 45 degree with respect to one of the polarizers to measure under crossed polarizers [8–11]. The unpolarized laser diode ($\lambda = 532$ nm) was used as a light source. The phase profiles of the LC lens are shown in Figs. 2(a) and 2(b). When $(V_1, V_2) = (0, 45V_{\text{rms}})$, the LC lens is a negative lens. When $(V_1, V_2) = (90 V_{\text{rms}}, 0)$, the LC lens is a positive lens. The phase profiles show concentric circles, but the number of rings of the negative lens is less than that of the positive lens. This also means the lens power of the positive lens in Fig. 2(b) is larger than the negative lens in Fig. 2(a). We can further calculate the lens power of the LC lens based on the phase profiles by Eq. (6) expressed as [18–20]:

$$P_{LC}(V) = \frac{2 \cdot N \cdot \lambda}{r^2}, \quad (6)$$

where N is the number of rings of the phase profile, λ is the wavelength ($\lambda = 532\text{nm}$), and r is the aperture size. The lens power as a function of applied voltage is shown in Fig. 2(c). In Fig. 2(c), black dots represent the lens power of the LC lens under different V_2 when $V_1 = 90 V_{\text{rms}}$, and red triangles represent the lens power of the LC lens under different V_1 when $V_2 = 45 V_{\text{rms}}$. The lens power can be switched from 0 to 19.9 Diopter (D or m^{-1}) under the operation of the positive lens when we apply a voltage of V_2 at $V_1 = 90 V_{\text{rms}}$. As to the lens power of negative lens, the measured power can be changed from -12.5 to 0 D when we apply a voltage of V_1 at $V_2 = 45V_{\text{rms}}$. The reason why we chose the fixed $V_2 = 45V_{\text{rms}}$ for negative lens and the fixed $V_1 = 90V_{\text{rms}}$ for positive lens is to keep the parabolic phase profile with applied voltage [18,19]. According to Fig. 2(c), the total change of the lens power of the LC lens is $19.9 + 12.5 = 32.4$ D.

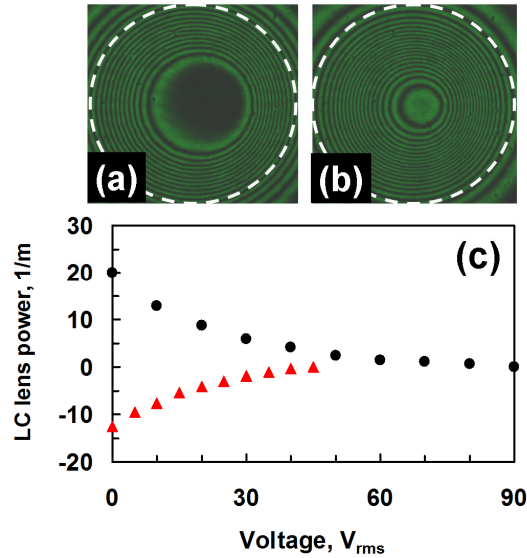


Fig. 2. Phase profile of the LC lens. (a) The LC lens is the negative lens at $V_1 = 0$, $V_2 = 45 V_{rms}$. (b) The LC lens is the positive lens at $V_1 = 90 V_{rms}$, $V_2 = 0$. (c) Lens power as a function of applied voltage. Black dots stand for the lens power as a function of applied voltage V_2 at $V_1 = 90 V_{rms}$. Red triangles stand for the lens power as a function of applied voltage V_1 at $V_2 = 45 V_{rms}$.

To further demonstrate the endoscopic system using a LC lens, we use a commercial endoscope (New Ken Technologies, Model: NK2458-OV7670-N/P-AWB-30-60 with 1/6" VGA CMOS Camera) provided by New Ken Technologies Co. Ltd. (Taiwan). The endoscope consists of arrays of LED light, an imaging lens module whose effective lens power (i.e. P_s) is 230 D, and a CMOS image sensor with 0.3 mega pixels. The endoscope was connected with a computer via an analog TV stick (Compro technology, VideoMate U2600F). The LC lens with a polarizer was attached to the imaging lens module. A resolution chart (USAF 1951) with a spatial frequency of 2.24 lp/mm was placed in front of the endoscope. The distance between the resolution chart and the LC lens is the objective distance. We recorded the images at different objective distances when the LC lens was applied different voltages and analyzed the recorded images. The images were converted to the spatial distribution of the brightness by using a software (Matlab). The contrast (C) of an image of the resolution chart was defined as [21]:

$$C = \frac{I_{max} - I_{min}}{I_{max} + I_{min}}, \quad (7)$$

where I_{max} and I_{min} were the maximum brightness and minimum brightness of the image, respectively. We then plotted the contrast as a function of objective distance at different applied voltages of the LC lens, as shown in Fig. 3. At $V_1 = V_2 = 0$, the contrast (C) increases and then decreases with the objective distance, as shown in red dots in Fig. 3. The maximum contrast is 0.84 at the objective distance of 43.2 mm. The objective distance for obtaining maximum contrast (C_{max}) depends on the lens power or focal length of the LC lens which is determined by the applied voltages. The sharpness of the image decreases when the object moves back-and-forth around the objective distance for obtaining maximum contrast. In our experiments, DOF is the distance when $C \geq 0.5C_{max}$ [21]. For $V_1 = V_2 = 0$, the DOF of the endoscopic system is around 30 mm (i.e. the objective distance is from 27 mm to 57 mm as $C \geq 0.5C_{max}$.) When $V_1 = 90V_{rms}$ and $V_2 = 0$ (black squares in Fig. 3), the LC lens acts as a

positive lens. The C_{\max} is 0.54 at the objective distance of 19.8 mm. When $V_1 = 0$ and $V_2 = 45V_{\text{rms}}$ (green triangles in Fig. 3), the LC lens acts as a negative lens. The C_{\max} is 0.76 at the objective distance of 56 mm. This means the endoscope can see the object further from 43.2 mm to 56 mm when the LC lens is a negative lens and see nearer from 43.2 mm to 19.8 mm when the LC lens is a positive lens. The C_{\max} decreases when the LC lens activated is because of the aberration of the LC lens. Improving the image properties can improve the C_{\max} [15]. Moreover, the DOF also changes with the objective distance. For $V_1 = 90V_{\text{rms}}$ and $V_2 = 0$, the DOF of the endoscopic system is around 14.6 mm (i.e. the objective distance is from 12.4 mm to 27 mm as $C \geq 0.5C_{\max}$). For $V_1 = 0$ and $V_2 = 45V_{\text{rms}}$, the DOF of the endoscopic system is around 38.8 mm (i.e. the objective distance is from 37.6 mm to 76.4 mm as $C \geq 0.5C_{\max}$). The DOF changes from 38.8 mm, 30 mm to 14.6 mm when the LC lens has a negative lens power of -12.5 D, zero lens power, and positive lens power of $+19.9$ D. Without a LC lens, the DOF of the endoscope is only 30 mm at the objective distance of 43.2 mm. Under the assistance of the LC lens, the endoscope can see the object located between 12.4 mm to 76.4 mm. As a result, we can enlarge the spatial depth perception of the object in the entire system (i.e. $76.4 - 12.4 = 64$ mm) by operating the LC lens with three discrete lens powers with three sets of applied voltages of (V_1, V_2) . Therefore, the function of the LC lens in the endoscopic system is not only to shift the objective distance, but also adjust the DOF. The spatial depth perception of the object is larger in the endoscope adopting a LC lens with three discrete lens powers. The concept is not just limited to three discrete lens powers and it also can be extended to more discrete lens powers or continuous lens power. In addition, other active optical lenses with discrete-focusing and fast-response properties can also be used in the endoscopic system, such as diffractive type of the LC lenses and the LC lens based on controllable polarizations [22,23]. To further enlarge the spatial perception of the system, enlarging the positive lens power and reducing the negative lens power are ways to go.

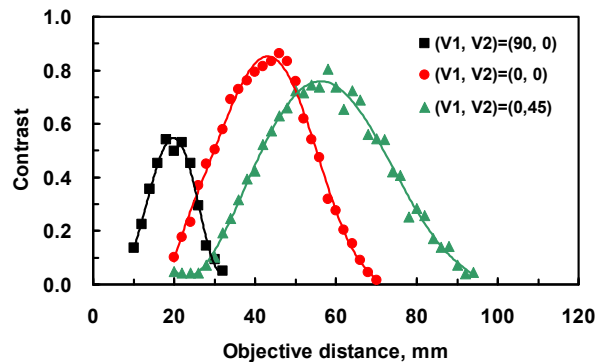


Fig. 3. The contrast as a function of the objective distance at $(V_1 = 0V_{\text{rms}}, V_2 = 0V_{\text{rms}})$ depicted as red dots, at $(V_1 = 90V_{\text{rms}}, V_2 = 0V_{\text{rms}})$ depicted as black squares, and at $(V_1 = 0V_{\text{rms}}, V_2 = 45V_{\text{rms}})$ depicted as green triangles. The lens powers of the LC lens at $(V_1 = 0V_{\text{rms}}, V_2 = 0V_{\text{rms}})$, $(V_1 = 90V_{\text{rms}}, V_2 = 0V_{\text{rms}})$, and $(V_1 = 0V_{\text{rms}}, V_2 = 45V_{\text{rms}})$ are 0, 19.9D, and -12.4 D, respectively.

From Fig. 3, the objective distance for C_{\max} can be adjusted by electrically adjusting the LC lens power and the DOF is also changed accordingly. In order to further investigate the objective distance for C_{\max} and DOF, we plotted the objective distance as a function of LC lens power when the contrast is maximum (black dots), and the near objective distance v.s. LC lens power and the far objective distance v.s. LC lens power when the contrast is half of maximum contrast, as shown in Fig. 4. In Fig. 4, the objective distance for C_{\max} changes from 56 mm to 19.8 mm when the LC lens power changes from -12.5 D to 19.9 D. The experimental results agree quite well with the theoretical prediction (grey dotted line) according to Eq. (1). In Fig. 4, the negative lens power helps the endoscope to see further and the positive lens

power helps the endoscope to see nearer. In Fig. 4, the far objective distance (76.4mm to 27mm) and the near objective distance (37.6mm to 12.4mm) decrease with the LC lens power. To obtain DOF, we subtracted the near objective distance from the far objective distance in Fig. 4 and obtained DOF. Then we plotted the DOF as a function of the LC lens power in Fig. 5. DOF decreases from 38.8 mm to 14.6mm when we increase the LC lens power. According to Eq. (1), we also plotted the DOF as a function of LC lens power in black line in Fig. 5 after putting the related parameters in the experiments: $P_s = 230$ D, $d_1 = 0.7$ mm, $d_2 = 3.83$ mm, $n = 1.5$. The experimental results and theoretical prediction are agreeable. As a result, we can electrically adjust the LC lens power to shift the objective distance from 56 mm to 19.8 mm. Moreover, DOF helps to enlarge the viewing range by extending the spatial depth perception. Therefore, the total viewing range or spatial depth perception is electrically tunable from 12.4 mm to 76.4 mm. We can continuously change the lens power by applied voltages or we can just adjust three discrete lens powers (i.e. -12.5 D, 0 D, and 19.9 D) of the LC lens to obtain the large viewing range. To enlarge the spatial depth perception, we can increase the tunable lens power of LC lens or reduce the effective aperture size of the entrance pupil of the endoscope system, as shown in Eq. (3). In addition, the C_{max} in Fig. 3 decreases with the LC lens power. This is because the high-order aberration of the LC lens increases with the lens power. We can improve the decrease of the C_{max} by improving the LC lens, such as the thickness of the buffering layer (glass substrate) and driving method [18,19].

The response time is also an important parameter of the electrically tunable endoscopic system by adopting a LC lens. When we switched the voltages from $(V_1, V_2) = (90V_{rms}, 0V_{rms})$ to $(V_1, V_2) = (0V_{rms}, 0V_{rms})$, the response time is around 4 sec. In order to improve the response time, we have to avoid the relaxation time of liquid crystals (i.e. null voltages). As a result, the response time is around 0.5 sec which is practical for applications when we switch the voltages from $(V_1, V_2) = (90V_{rms}, 0V_{rms})$ to $(V_1, V_2) = (90V_{rms}, 90V_{rms})$ in order to operate the LC lens from 19.9 D to 0D. The driving voltage of the LC lens can be reduced ($<5 V_{rms}$) by adding extra-polymeric layers or improving the structure of the LC lenses [24]. As to the increase of light efficiency, we can develop polarization independent LC lenses to remove the polarizer based on the double-layered structure, the residual phase structure, the mixed type phase modulation, and the optically isotropic structure [8, 13, 25–35].

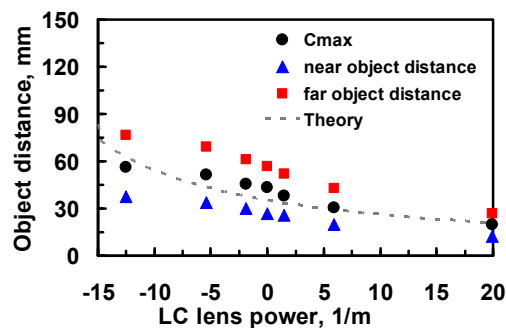


Fig. 4. Objective distance as a function of LC lens power when the contrast is maximum (black dots). Blue triangles and red squares represent the near objective distance and far objective distance when the contrast is half of maximum contrast. Grey dotted line stands for the theoretical prediction for the maximum contrast according to Eq. (1).

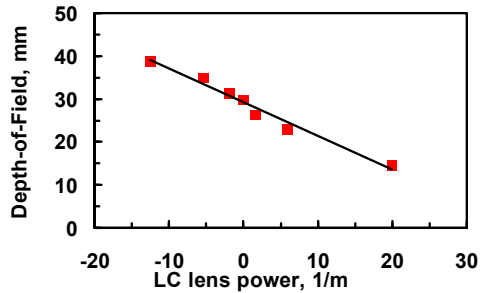


Fig. 5. DOF as a function of LC lens power for the experiments (red squares) and theoretical prediction (black line). DOF is defined as the difference between the near objective distance and far objective distance in Fig. 4.

The image performances of the endoscopic system adopting a LC lens are shown in Figs. 6(a)-6(c). At $(V_1, V_2) = (0V, 0V)$, the lens power of the LC lens is zero and the DOF (δ_1) was 30 mm. The endoscopic system can only see the range around 57 mm to 27 mm, as shown in Fig. 6(a). When the LC lens is on at $(V_1, V_2) = (90V, 0V)$, the lens power of the LC lens is positive $\sim +19.9$ D and the DOF (δ_2) was 14.6 mm, the endoscopic system can see nearer from 27 mm to 12.4 mm, as shown in Fig. 6(b). When $(V_1, V_2) = (0V, 45V)$, the lens power of the LC lens is negative ~ -12.5 D and the DOF (δ_3) was 38.8 mm, the endoscopic system can see further from 76.4 mm to 37.6 mm, as shown in Fig. 6(c). Under adjustment of the LC lens power, the total viewing range or total spatial depth perception of the endoscopic system is from 76.4 mm to 12.4 mm, which means the DOF is extended to 64 mm. Compared to the conventional one without LC lens, the DOF is 2x improved by three discrete adjustment of the LC lens power. In Fig. 2, the lens profile does not show perfect symmetry related to the image quality of the LC lens. In fact, we had measured the modulation transfer function (MTF) for the same structure of the LC lens in our previous works, the LC lens shows high spatial resolution with the cutoff frequency > 280 lp/mm compared to that of human eyes with the cutoff frequency < 60 lp/mm [10].

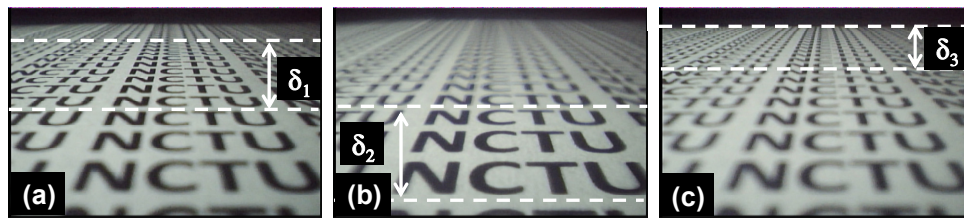


Fig. 6. The image performances of the endoscopic system. (a) The lens power of the LC lens is zero and the DOF $\delta_1 = 30$ mm. The objective distance is from 57mm \sim 27mm. (b) The lens power of the LC lens is $+19.9$ D and the DOF $\delta_2 = 14.6$ mm. The objective distance is from 27mm \sim 12.4mm. (c) The lens power of the LC lens is -12.4 D and the DOF $\delta_3 = 38.8$ mm. The objective distance is from 76.4mm \sim 37.6mm.

4. Conclusion

We demonstrated an electrically tunable endoscopic system by adopting a LC lens with a large spatial depth perception. Both of the objective distance and the corresponding DOF of the endoscopic system can be adjusted by the two mode operation of LC lens: positive lens and negative lens. Instead of continuously changing the focal lengths of the LC lens, selecting three discrete tunable focal lengths of the LC lens can help the endoscopic system to see the object in a scene from 76.4 mm to 12.4 mm which is good enough for medical applications (~ 30 mm - 60 mm). The viewing range or spatial depth perception is 2x improved compared to the one without the tunable focusing LC lens (from 30 mm to 64mm). The optical mechanism of DOF in such an electrically tunable endoscopic system is discussed as well. The advantages

of the LC lens is small size, and low power consumption ($\sim 4 \mu\text{W}$) [36]. To demonstrate the concept, we simply attached the LC lens with the imaging lens which is actually a lens module consisting of several pieces of solid lenses. For the practical applications, the LC lens should be combined with the lens module and redesign the lens module in order to lower the aberration and the chromatic aberration. The concept we proposed not only applies to LC lenses but also can apply to other active optical elements or phase modulators. We believe this study provides a guideline to help the researchers and engineers to develop the electrically tunable endoscopic system for the industrial and medical applications.

Acknowledgments

The authors are indebted to Mr. Ming-Syuan Chen and Mr. Yu-Jen Wang for technical assistance, and Mr. Paul Chen in New Ken Technologies Co. Ltd. for providing the endoscope. This research was supported mainly by Liqxtal Technology Inc. and partially by the National Science Council (NSC) in Taiwan under the contract no. NSC 101-2112-M-009-011 -MY3.